Antifungal Activity of TiO₂/Ag Nanoparticles under Visible Light Irradiation

Nahzim Rahmat[*], Endang Tri Wahyuni, and Adhitasari Suratman

Department of Chemistry, Faculty of Mathematics and Natural Sciences, Universitas Gadjah Mada,
Sekip Utara, Yogyakarta 55281, Indonesia

Abstract: *The doping of TiO₂ by Ag(I) from $[Ag(S_2O_3)_2]^{3-}$ contained in radiophotography wastewater by photoreduction method has been performed. TiO₂/AgNPs photocatalyst was examined for its activity as an antifungal material for the inhibition of* C. albicans *in water under visible light irradiation. In the doping process, the weight of TiO₂ was varied to obtain TiO₂/AgNPs with different amounts of Ag. The TiO₂/AgNPs samples were characterized by using FTIR, SRUV, TEM, SEM-EDX, and XRD methods. The antifungal test was carried out by disc diffusion method under visible light irradiation, wherein the amount of Ag-doped on TiO₂, the dose of TiO₂/AgNPs, and the irradiation time were optimized. The research results indicated that the antifungal activity of TiO₂/AgNPs in inhibiting* C. albicans *has been successfully prepared. The highest inhibition was achieved by using 0.5 g/L of TiO₂/AgNPs (I), at 5 h of irradiation time.*

Keywords: *TiO₂/Ag; antifungal;* C. albicans; *visible light; nanoparticle*

■ INTRODUCTION

Yeast is a significant component of the microbiota of most natural aquatic ecosystems. The majority of these organisms have no known human health effects. However, a small number of species, primarily within the anamorphic genus *Candida*, are important opportunistic pathogens. *Candida albicans* (*C. albicans*) is an opportunistic pathogen that has a potential impact to increase the risks of waterborne diseases. The presence of *C. albicans* in recreational water and public pools [1-2] requires inclusive attention due to the high risk of infection by the carrier to the human body.

Various methods have been carried out to disinfect water from *C. albicans*, such as conventional methods, ozone water treatment, photo-Fenton, and photocatalysis using TiO₂ under UV light irradiation. The conventional method is a simple method that involves the addition of hypochlorite [Ca(OCl)₂]. This chemical is only effective at pH 7 and temperatures of 23–25 °C. The residue of this chemical has mutagenic and carcinogenic properties when it enters the human digestive tract [3].

The ozone water treatment method is quite effective in killing *C. albicans*, but the operational and installation

costs are expensive [4]. The photo-Fenton method has been proven to kill the *Fusarium solani* fungus [5], but this method still uses UV as a source of radiation, even though the sun only has 3–4% of UV radiation. Photocatalysis using TiO₂ under UV light irradiation has been proven by Tathdil et al. [6] to eradicate *C. albicans*, but the use of TiO₂ was ineffective in visible light regions.

Ag-doped TiO₂ has been proven to increase TiO₂ activity in the visible region by the photoreduction method [7]. Radiophotography wastewater has been reported as a cheap source of Ag(I) that contains $[Ag(S_2O_3)_2]^{3-}$ [8]. The effort to replace expensive AgNO₃ as an Ag precursor, as well as to convert the toxic $[Ag(S_2O_3)_2]^{3-}$ in wastewater into more valuable material, is proposed in this work. On the other hand, radiophotography wastewater was chosen as the source of Ag(I) to support sustainable development goals as well. The synergistic effect between Ag nanoparticles and OH radicals that are produced by TiO₂ after irradiation of UV light increases the antifungal ability of TiO₂/AgNPs.

The ability of TiO₂/Ag nanoparticles (TiO₂/AgNPs) to eradicate microorganisms has not been tested yet on *C. albicans*. Therefore, this study aims to determine the

inhibition of TiO$_2$/AgNPs on the growth of *C. albicans* by disc diffusion method. In this study, photocatalyst dosage optimization and variation of visible light irradiation time were carried out.

■ EXPERIMENTAL SECTION

Materials

The radiophotography wastewater was collected from the Mitra Paramedika Hospital of Yogyakarta, Indonesia, and was used as a source of Ag(I). The silver standard solution, TiO$_2$ powder, Nutrient Broth (NB) powder, and Sabouraud Dextrose Agar (SDA) powder were purchased from Merck. Liquid cultures of *Candida albicans* ATCC® 10231 were obtained from the Laboratory of the Microbiology Department, Faculty of Medicine, UGM.

Instrumentation

A set of the photoreduction apparatus with UV Lamp (Black Light Blue 40 W, 220 V, intensity = 0.040 lx) was used for TiO$_2$/Ag preparation by following the procedure previously reported [8]. Atomic Absorption Spectroscopy/AAS (Perkin-Elmer type 3110), Infra-Red/IR (Shimadzu Prestige 21), Specular Reflectance Ultra Violet/SRUV (Pharmaspec UV 1700), Transmission Electron Microscopy/TEM (JEOL JEM-1400), SEM-EDX (JEOL JSM-6510LA) and X-ray Diffraction/XRD (Shimadzu 6000D) machines were applied for the analysis and characterization of the photocatalyst products. A set of irradiation reactor with a UV lamp (Philips TLD 18 W, 220 V cool daylight, intensity 4750 lx) and visible lamp (Philips TLD 18 W, 220 V cool daylight, intensity = 4750 lx) with wavelengths of 350–400 nm, calliper, autoclave (Hirayama HA-300 MD), micropipette (Socorex), lux meter (mobiken illuminance meter LX2), and incubator (Thelco Oven 4-E-2 Cat No. 31483) were applied for the analysis and assay of the antifungal activity.

Procedure

Analysis of the radiophotography wastewater sample

The Ag(I) content in the sample before and after photoreduction was determined by AAS method. The amount of Ag reduced and incorporated on TiO$_2$ structure was calculated using the following formula:

$$C_r = \frac{C_0 - C_{ur}}{W} \times V$$

C$_r$ = The amount of Ag(I) reduced (mg g^{-1})
C$_0$ = The concentration of Ag(I) in the wastewater before photoreduction (mg L^{-1})
C$_{ur}$ = The concentration of Ag(I) in the wastewater after photoreduction (mg L^{-1})
W = The weight of TiO$_2$ used in photoreduction (mg)
V = The volume of wastewater (L)

From the AAS analysis, it was found that the concentration of Ag(I) in the radiophotography wastewater was 1502 mg/L.

Preparation of TiO$_2$/AgNPs photocatalyst

TiO$_2$ with the weight of 150, 300, and 450 mg were added to separate flasks. Every flask contained 50 mL of radiophotography wastewater and was diluted until 250 mL. The flasks were placed into a sonicator for 1 h and then placed in the photoreduction apparatus. The flasks were exposed to a 40 W UV lamp and were kept stirred with magnetic stirrers at a spin rate of 1500 rpm for 24 h. The product of this process was filtered by using Whatman #42 filter paper to get the solid and filtrate products. The solids were dried at 60 °C and labeled as TiO$_2$/Ag(150), TiO$_2$/Ag(300), and TiO$_2$/Ag(450), corresponding to the weight of TiO$_2$ that was used. The filtrates were analyzed using AAS to determine the Ag(I) content in the wastewater sample before and after photoreduction.

Characterization of the prepared TiO$_2$/AgNPs photocatalyst

The photocatalysts produced were characterized by FTIR, SRUV, XRD, SEM-EDX, and TEM. For FTIR analysis, the solids were made into pellets with KBr and were scanned from 400 to 4000 cm^{-1}. The SRUV spectra were taken from the wavelength of 200 to 880 nm. The XRD patterns were recorded using Cu-Kα as the source of radiation with a step of 0.017° and scanning from 5 to 90° (2-theta). The TEM images were shot using copper grids by loading the aqueous suspension at a suitable concentration. The EDX spectra were recorded on JSM-

6510LA (JEOL), equipped with EDX JEOL detector and Analysis Station Software (JEOL).

Antifungal assay by TiO₂/AgNPs photocatalyst

The antifungal assay by one of the TiO$_2$/AgNPs photocatalyst was carried out by in vitro agar disc diffusion method. All apparatus used were sterilized. A few of the liquid cultures of *C. albicans* were diluted and regrown in nutrient broth (NB) and then incubated for 24 h at 37 °C. The Sabouraud Dextrose Agar 14% with the weight of 6.5 g was dissolved in 100 mL distilled water and then placed into an autoclave to be sterilized at 121 °C and 15 psi for 15 min. The solution was poured into a petri dish then cooled to obtain an agar form. NB was applied and covered on the whole surface area of the agar media (test media) using a sterile cotton swab. The sample (20 μL, 0.3 g/L), sterile distilled water as a negative control which was irradiated for 1 h, and ampicillin disc as a positive control (10 μg) were applied to the test media. This petri dish was incubated for 24 h at 37 °C. The diameter of the inhibition zone was measured using callipers to determine the antifungal activity. The inhibition zone was measured by reducing the overall diameter (paper disc + inhibition zones) with the paper disc diameter. The same procedure was carried out for the visible light irradiation time (1, 3, 5, 7, and 10 h) and the dose variation of TiO$_2$ and TiO$_2$/AgNPs (0.1, 0.3, 0.5, 0.7, and 1 g/L),

■ RESULTS AND DISCUSSION

The photodecomposition of the thiosulfate complex [Ag(S$_2$O$_3$)$_2$]$^{3-}$ can be proceeded through photoreduction under UV light irradiation. This process is catalyzed by the TiO$_2$ photocatalyst. When TiO$_2$ absorbs UV light, one electron (e$^-$) is excited from the valence band into the conduction band while leaving a hole (h$^+$) which is a positively charged radical [13]. The excited electron can react with Ag$^+$ which would then be reduced to form Ag^o [10]. The reactions are represented by Eq. (1), (2), and (3). At the same time, the hole (h$^+$) can react with a water molecule to form a hydroxide radical (•OH) and a proton (H$^+$) (Eq. (4)). [Ag(S$_2$O$_3$)$_2$]$^{3-}$ was believed to be oxidized by •OH to form S^0 and SO$_4$$^{2-}$ as seen in Eq. (5) [14].

$$TiO_2 + UV\ light \rightarrow TiO_2(e^- + h^+) \tag{1}$$

Fig 1. The influence of the TiO$_2$ weight on the amount of Ag^0 formed in TiO$_2$/AgNPs

$$\left[Ag(S_2O_3)_2\right]^{3-} \rightleftarrows Ag^+ + 2S_2O_3^{2-} \tag{2}$$

$$Ag^+ + e^- \rightarrow Ag^0 \tag{3}$$

$$H_2O + h^+ \rightarrow H^+ + \cdot OH \tag{4}$$

$$S_2O_3^{2-} + \cdot OH \rightarrow H^+ + SO_4^{2-} + S^0 \tag{5}$$
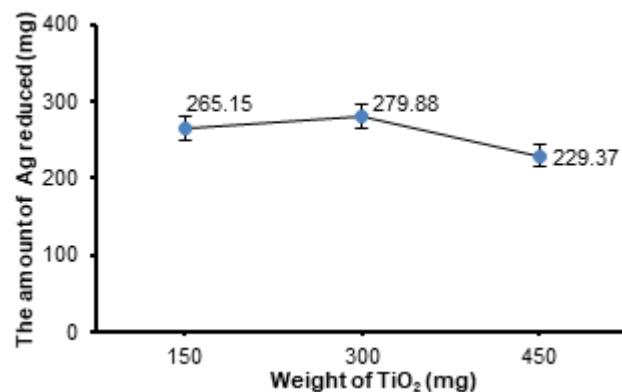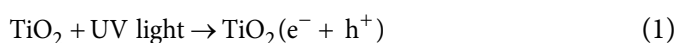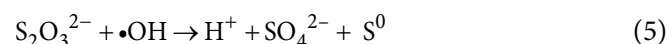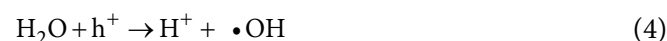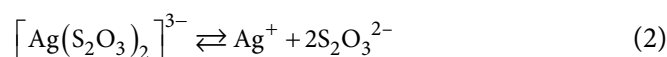
In this research, the study on the effect of TiO$_2$ weight toward the amount of Ag^0 formed in the TiO$_2$/AgNPs photocatalyst was carried out. Fig. 1 exhibits the amount of Ag(I) reduced from wastewater to form Ag^0 that was incorporated in the TiO$_2$/AgNPs photocatalyst, in which the amount of TiO$_2$ introduced was varied. In Fig. 1, a considerable increase of Ag(I) reduced on the TiO$_2$ surface was observed when the initial amount of TiO$_2$was raised from 150 to 300 mg. This phenomenon was well accepted due to the increased amount of Ag(I) when it captured the release of more electrons which originated from TiO$_2$, eventually causing the increase of the reduced Ag(I). However, when the weight of TiO$_2$ was increased, the amount of reduced Ag(I) decreased. Apparently, the larger amount of TiO$_2$ which exceeded 450 mg, had implicated the turbidity level of the mixture, thereby inhibiting UV light entering the mixture. Consequently, the contact opportunity between UV light and Ag$^+$ decreased, thereby decreasing the amount of Ag(I) reduced.

Characterization of TiO₂/AgNPs Photocatalyst

FTIR

Fig. 2 shows the FTIR spectra of TiO$_2$/AgNPs with various amounts of reduced Ag(I) (279.88, 265.15, and

229.37 mg) prepared by using different TiO_2 weights (150, 300, and 450 mg). For the amount of reduced Ag(I) of 279.88 mg, the notation used was TiO_2/AgNPs (I), while TiO_2/AgNPs (II) and TiO_2/AgNPs (III) denoted the amount of reduced Ag(I) of 265.15 mg, and 229.37 mg, respectively. The strong peaks of anatase TiO_2 were seen at 532, 678, 1635, and 3433 cm^{-1}, which corresponds to the Ti–O–Ti stretching, Ti–O–Ti bending, O–H bending of water, and O–H stretching of Ti–O–H, respectively [8,12]. The spectra for all TiO_2/AgNPs samples showed similar peaks with some observable shifts. The peak shifted from 532 to 524 cm^{-1}, 678 to 671 and 655 cm^{-1}, as well as from 1635 to 1627 cm^{-1}. This may be caused by the interaction between Ti–O with Ag ions. According to the fundamental transverse optical phonon mode [13-14], the loading of Ag nanoparticles on the surface of TiO_2 should result in downward shifts of the peaks.

XRD data

The structure and the crystallization of TiO_2 and TiO_2/AgNPs were confirmed by using X-ray powder diffraction (XRD, Fig. 3). The XRD patterns of TiO_2 and TiO_2/AgNPs was taken in the range of 3–80°. The characteristic peaks of anatase TiO_2 appeared at 2θ values of 25.13°, 37.59°, 47.86°, 53.69°, 54.90°, 62.54°, 68.59°, 70.16° and 74.88°, and are shown in Fig. 3(a). These peaks were confirmed with JCPD Card No. 21-1272 that were attributed to the diffraction of anatase TiO_2 [9].

Generally, the XRD patterns of TiO_2/AgNPs samples with different Ag loads were seen to be almost the same as that of pure TiO_2, however, Fig. 3(b), 3(c), and 3(d) show that the peak intensities of the TiO_2/AgNPs samples were lower than pure TiO_2 (Fig. 3(a)). This indicates that Ag^0 loading only had a small influence (there was almost no effect) [4,15]. The low intensity shown in Fig. 3(b), represented the TiO_2/AgNPs (I) sample that had the highest Ag^0 content.
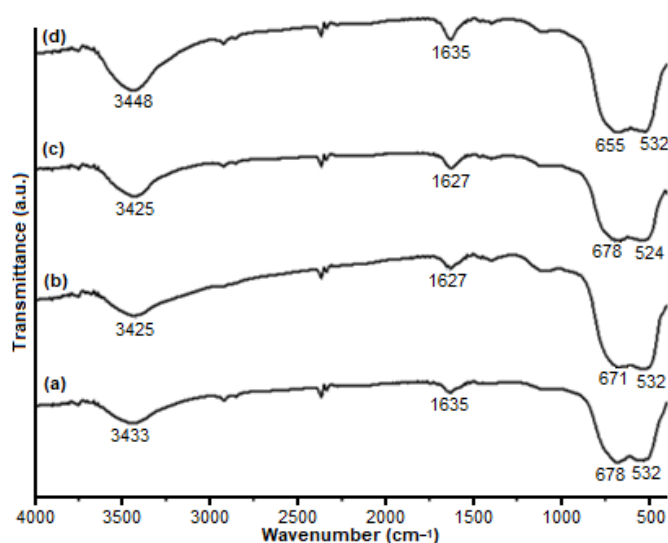
Fig 2. FTIR spectra of (a) TiO_2, (b) TiO_2/AgNPs (III), (c) TiO_2/AgNPs (II), and (d) TiO_2/AgNPs (I)
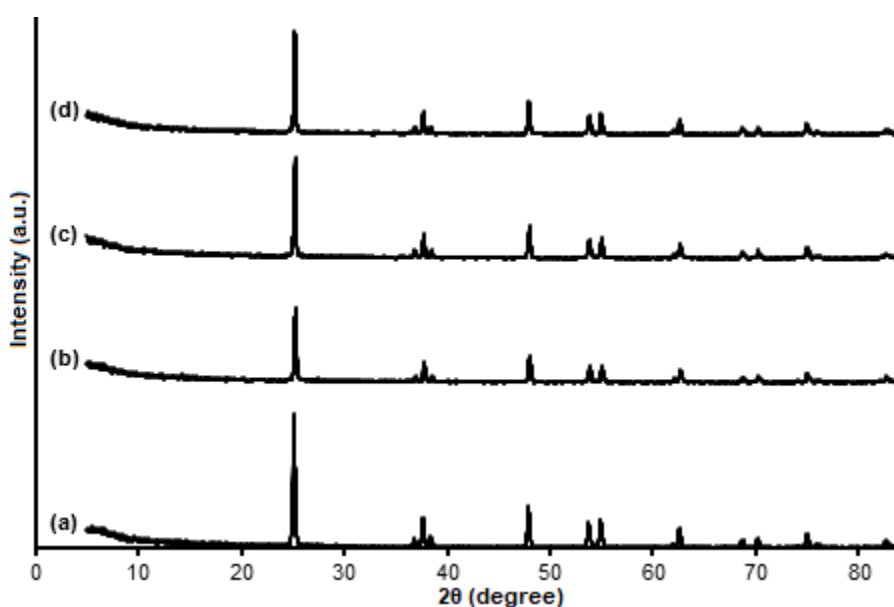
Fig 3. XRD patterns of (a) TiO_2, (b) TiO_2/AgNPs (I), (c) TiO_2/AgNPs (II), and (d) TiO_2/AgNPs (III)

This indicated that Ag^0 had covered most of the surface of TiO_2, reducing the intensity of the X-ray diffraction.

The TEM images

The TEM images of TiO_2 and TiO_2/AgNPs samples with various Ag^0 content are displayed in Fig. 4. Fig. 4(a) shows that the TiO_2 surface was clean and mostly grey [12]. Fig. 4(b), 4(c), and 4(d) show the presence of dark layers in the form of small spheres on the surface of TiO_2 which was likely Ag [11,16-19]. These images also show that the Ag loaded on the surface of TiO_2 were already in nanoparticle size.

EDX data analysis was performed on TiO_2 and TiO_2/AgNPs to determine the content and composition of the elements before (TiO_2) and after loading (TiO_2/Ag). Based on the EDX data analysis, as shown in Table 1, it can be seen that there was a mass of Ag after the loading process. This indicates that the loading of Ag on the surface of TiO_2 was successful. This data can be used to support the TEM images and confirm that the darkest layer in the form of small spheres that appeared on the surface of TiO_2 was likely to be Ag [20]. TiO_2/AgNPs (I) photocatalyst had a higher Ag^0 content compared to the
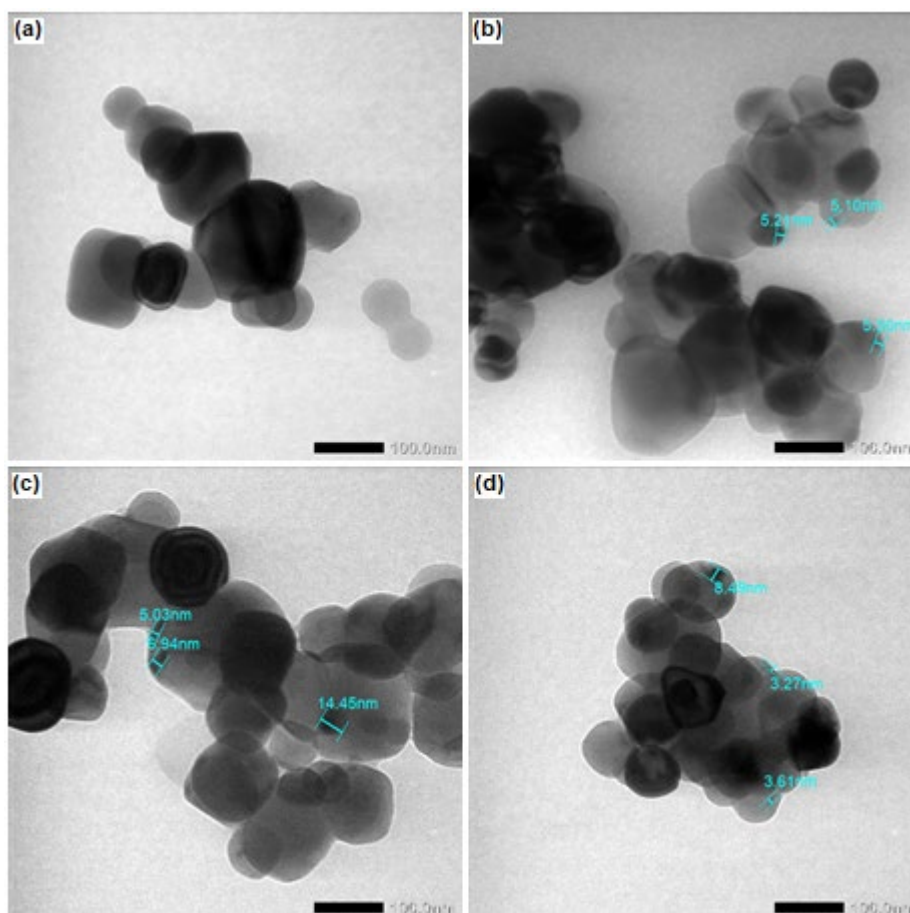
Fig 4. TEM images of (a) TiO_2, (b) TiO_2/AgNPs (I), (c) TiO_2/AgNPs (II), and (d) TiO_2/AgNPs (III)

Table 1. EDX data analysis of TiO_2, TiO_2/AgNPs (I), TiO_2/AgNPs (II), and TiO_2/AgNPs (III)

Element	TiO_2 (Mass %)	TiO_2/AgNPs (I) (Mass %)	TiO_2/AgNPs (II) (Mass %)	TiO_2/AgNPs (III) (Mass %)
O	52.28	48.45	51.67	53.03
Ti	47.72	44.75	43.79	43.92
Ag	-	6.80	4.54	3.04

other photocatalysts. These results are in agreement with the FTIR and XRD results.

SRUV spectra

The SRUV spectra of the prepared photocatalysts are shown in Fig. 5. The peak absorbance of TiO_2 was found at 381.94 nm, which is in the UV region. Meanwhile, the peak absorbance of the TiO_2/AgNPs samples shifted into the visible region. Calculation using the peak absorbance of the SRUV data provided band gap energies as presented in Table 2.

The band gap energies of TiO_2/AgNPs became lower than TiO_2. This indicated that Ag nanoparticles were loaded on the surface of TiO_2, so that the gap between the valence and conduction bands was narrowed. The photocatalyst TiO_2/AgNPs (I) had the smallest band gap energy compared to the other photocatalysts. This implied that the size of the Ag^0 particles was small and had the best particle distribution, so they can ideally be loaded on the surface of TiO_2. The band gap energy of TiO_2/AgNPs (II) was slightly greater than TiO_2/AgNPs (I) due to less Ag^0 content [21]. For TiO_2/AgNPs (III), the band gap energy was higher than the others. This indicates that the amount of Ag^0 loaded on the surface of TiO_2 was less than the other photocatalysts.

Antifungal Activity of TiO₂/AgNPs

Antifungal activity of TiO₂ and TiO₂/AgNPs under visible and UV light

Based on the results of the SRUV analysis, the lowest band gap energy was owned by TiO_2/AgNPs (I).

Therefore, this photocatalyst was tested for its antifungal activity. Fig. 6(a) shows that the TiO_2/AgNPs was active under visible light. This can be seen from the inhibition zone diameter, although it was still categorized as weak [22]. This barrier was probably derived from Ag^0 which
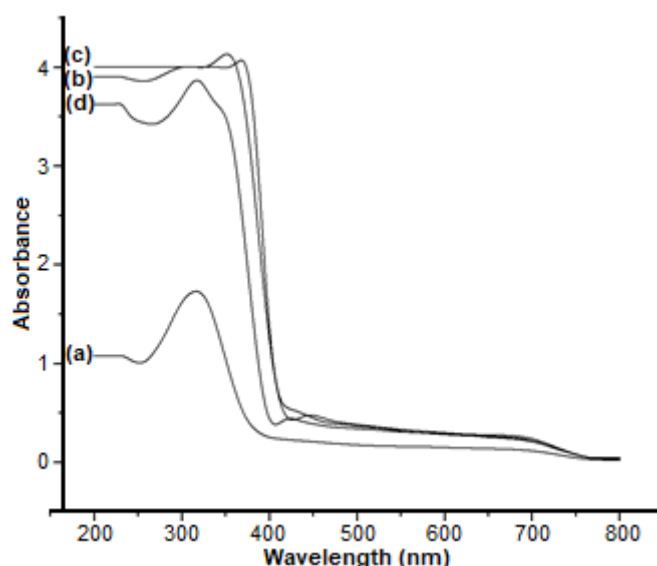
Fig 5. SRUV spectra of (a) TiO_2, (b) TiO_2/AgNPs (I), (c) TiO_2/AgNPs (II), and (d) TiO_2/AgNPs (III)

Table 2. The band gap energy of the titania-based photocatalysts

Photocatalyst	λm (nm)	Eg (eV)
Un-doped TiO_2	381.94	3.25
TiO_2/AgNPs (I)	412.70	3.00
TiO_2/AgNPs (II)	410.36	3.02
TiO_2/AgNPs (III)	397.31	3.12
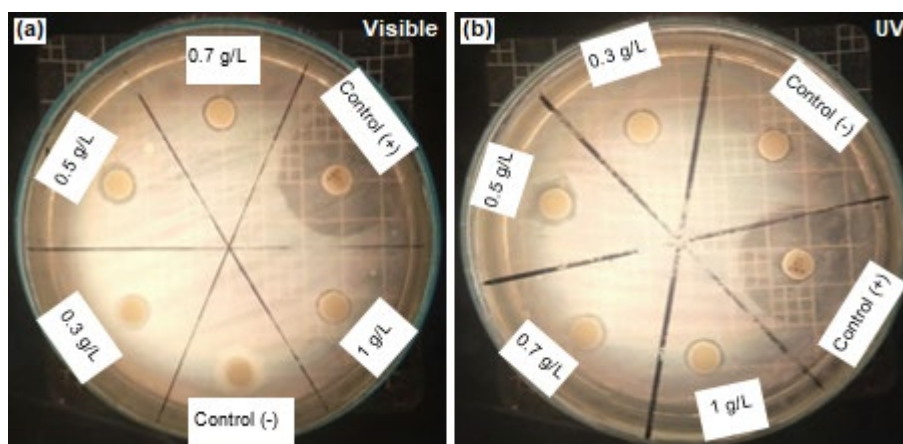
Fig 6. The inhibition zone of TiO_2/AgNPs in UV and visible light irradiation for 5 h on the *C. albicans*

damaged the fungal cell wall. TiO$_2$ photocatalysts are inactive under visible light because the visible light energy is lower than the energy gap of the TiO$_2$ band.

The antifungal activity of TiO$_2$/AgNPs was also tested under UV light (Fig. 6(b)) which showed a medium categorized inhibition zone diameter [22]. This suggests that the diameter of the inhibition zone under UV irradiation was wider than under visible light because there were some inhibitory mechanisms that occured, namely those derived from OH radicals and Ag^0 that damaged the fungal cell wall [23]. TiO$_2$ is active under UV light. This was indicated from the presence of the inhibition zone diameters, although they were still categorized as weak [22]. This barrier was probably derived from the reaction mechanisms of OH radicals that damaged the fungal cell wall. Observational data are presented in Fig. 7.

The 0.5 g/L dose was chosen for further experiments due to its antifungal activity. Actually, the other samples (0.3, 0.7, and 1 g/L) under visible light (except TiO$_2$ sample) and UV light also had inhibition activity. However, the most significant inhibition activity was at the dose of 0.5 g/L. This meant that 0.5 g/L was the ideal dose in this experiment. At a dose of 0.1 g/L, there was no inhibition zone, but at higher doses (0.3–1 g/L) the antifungal activity was independent of the catalyst concentration, due to the screening effect produced by the excess of suspended particles which resulted in an inefficient absorption of light by the photocatalyst [8,21].

Various irradiation times (1–10 h) were carried out in this research. At more than 5 h of irradiation, the antifungal activity was no longer dependent on the time irradiation, due to the saturation of the photocatalyst solution which resulted in an inefficient absorption of light [8]. Meanwhile, the irradiation time of 1 and 2 h were observed as well, yet there was no inhibition zone at all. Therefore, the optimum irradiation time was determined at 5 h.

The effect of irradiation time on the antifungal effectiveness of TiO$_2$/AgNPs

The effect of irradiation time using visible and UV light on the antifungal activity of TiO$_2$/AgNPs at a dose of 0.5 g/L is shown in Fig. 8. At a dose of 0.5 g/L, the

irradiation intensity that enters the mixture, in both the UV light and the visible light, was sufficient. On the other hand, the availability of OH radicals and Ag nanoparticles to target the large number of fungi was significant. The longer the irradiation time, the wider the diameter of the inhibition zone that occurs. A shorter irradiation time formed only a small amount of OH radicals, so contact with the fungal wall became less effective and the ability to eradicate the fungus decreased.

For a relatively longer time, the production of OH radicals reached optimum results, in which more OH radicals came in contact with *C. albicans*. This fact was indicated by the widening of the diameter of the inhibition zone. However, when the irradiation time was
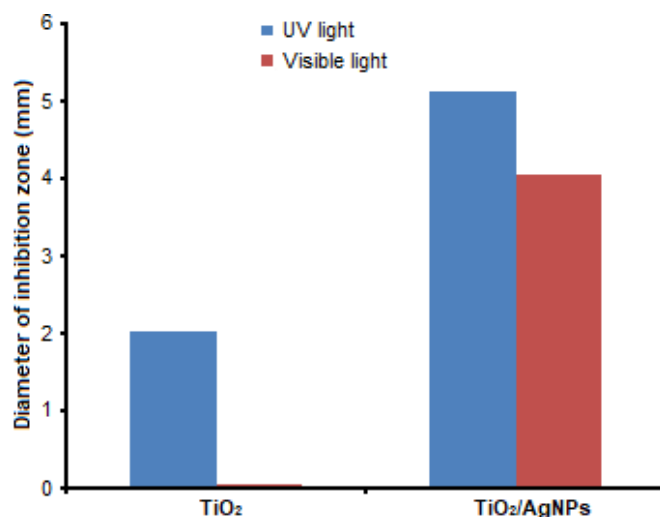
Fig 7. Antifungal activity of TiO$_2$ and TiO$_2$/AgNPs with 0.5 g/L of the doses on the irradiation for 5 h
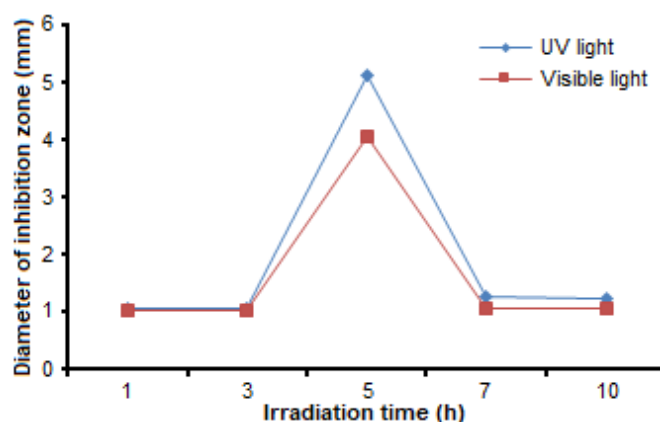
Fig 8. The effect of irradiation time on the antifungal activity of TiO$_2$/AgNPs with 0.5 g/L of the doses
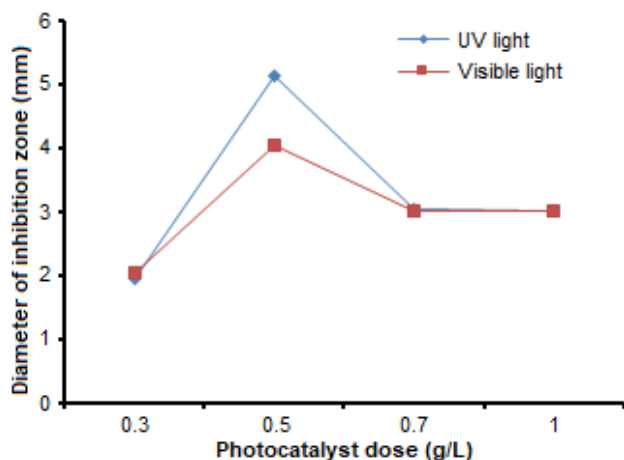
Fig 9. The effect of TiO$_2$/AgNPs photocatalyst dosage on antifungal activity of *C. albicans* with irradiation time for 5 h

further increased, the antifungal activity decreased as indicated by the decrease in the inhibition zone diameter. This phenomenon was caused by the occurrence of saturation on the surface of the photocatalyst, thereby reducing the ability of the photocatalyst to inhibit fungal growth [8]. The inhibition zone diameter under UV light appeared wider than under the visible light since it was not only Ag^0 that attacked the fungal cell wall, but also joined by OH radicals. Thus, there was a synergistic effect between Ag^0 and OH radical which increased the antifungal activity of TiO$_2$/AgNPs photocatalyst under UV light.

The effect of the photocatalyst dose on the antifungal effectiveness of TiO$_2$/AgNPs

The effect of the photocatalyst dose on the antifungal activity of TiO$_2$/AgNPs under 5 h of irradiation is shown in Fig. 9. When the dosage of the photocatalyst was higher, the diameter of the inhibition zone was wider. At low doses, the availability of Ag^0 was small. This caused the photocatalyst contact with *C. albicans* to be less effective, so the ability to eradicate the *C. albicans* was low. When the dose was increased, the amount of Ag^0 also increased; so that contact between the photocatalyst and *C. albicans* was more effective and the antifungal activity became higher. This was indicated by the widening of the inhibition zone diameter compared to the previous dose.

At higher photocatalyst dose, the number of photocatalyst particles in the solution also increased. This caused the solution to become turbid, causing obstruction

of visible radiation or UV light that enter the solution [8]. This phenomenon is known as the shadowing or screening effect [21,24]. This effect resulted in the inactivation of the photocatalyst particles thereby reducing its antifungal ability. These results are similar to the research of Wahyuni et al. [8] in which shadowing or screening effect also caused the antibacterial ability of TiO$_2$/AgNPs in killing *E. coli* to be reduced.

■ CONCLUSION

It can be concluded that the Ag^0 nanoparticles had been successfully loaded on TiO$_2$ by photocatalytic reduction of [Ag(S$_2$O$_3$)]$_2^{3-}$ contained in the radiophotography wastewater under UV light. AgNPs-doped TiO$_2$ was found to lose crystallinity and at the same time shifted the optical absorption into visible light. The highest inhibition was achieved by using 0.5 g/L of TiO$_2$/AgNPs (I), with 5 h of irradiation time.

■ ACKNOWLEDGMENTS

■ REFERENCES

[1] Amala, S.E., and Aleru, C.P., 2016, Bacteriological quality of swimming pools water in Port Harcourt Metropolis, *Nat. Sci.*, 8 (3), 79–84.

[2] Brinkman, N.E., Haugland, R.A., Wymer, L.J., Byappanahalli, M., Whitman, R.L., and Vesper, S.J., 2003, Evaluation of a rapid, quantitative real-time PCR method for enumeration of pathogenic *Candida* cells in water, *Appl. Environ. Microbiol.*, 69 (3), 1775–1782.

[3] Lubbers, J.D., Chauan, S., and Bianchine, J.R., 1982, Controlled clinical evaluations of chlorine dioxide, chlorite, and chlorate in man, *Environ. Health Perspect.*, 46, 57–62.

[4] Cesar, J., Sumita, T.C., Junqueira, J.C., Jorge, A.O.C., and do Rego, M.A., 2012, Antimicrobial effects of ozonated water on the sanitization of dental instruments contaminated with *E. coli, S.*

aureus, C. albicans, or the spores of *B. atrophaeus, J. Infect. Public Health,* 5 (4), 269–274.

[5] Polo-López, M.I., Castro-Alférez, M., Oller, I., and Fernández-Ibáñez, P., 2014, Assessment of solar photo-Fenton, photocatalysis, and H_2O_2 for removal of phytopathogen fungi spores in synthetic and real effluents of urban wastewater, *Chem. Eng. J.,* 257, 122–130.

[6] Tatlıdil, I., Sökmen, M., Breen, C., Clegg, F., Buruk, C.K., and Bacaksiz, E., 2011, Degradation of *Candida albicans* on TiO_2 and $Ag-TiO_2$ thin films prepared by sol–gel and nanosuspensions, *J. Sol-Gel Sci. Technol.,* 60 (1), 23–32.

[7] Wahyuni, E.T., Roto, R., and Prameswari, M., 2019, Antibacterial activity of TiO_2/Ag-nanoparticle under visible light, *Mater. Sci. Forum,* 948, 33–42.

[8] Wahyuni, E.T., Roto, R., Novarita, D., Suwondo, K.P., and Kuswandi, B., 2019, Preparation of TiO_2/AgNPs by photodeposition method using Ag(I) present in radiophotography wastewater and their antibacterial activity in visible light irradiation, *J. Environ. Chem. Eng.,* 7 (4), 103178.

[9] Abbad, S., Guergouri, K., Gazaout, S., Djebabra, S., Zertal, A., Barille, R., and Zaabat, M., 2020, Effect of silver doping on the photocatalytic activity of TiO_2 nanopowders synthesized by the sol-gel route, *J. Environ. Chem. Eng.,* 8 (3), 103718.

[10] Huang, M., Tso, E., Datye, A.K., Prairie, M.R., and Stange, B.M., 1996, Removal of silver in photographic processing wastewater by TiO_2-based photocatalysis, *Environ. Sci. Technol.,* 30 (10), 3084–3088.

[11] Sontakke, S., Mohan, C., Modak, J., and Madras, G., 2012, Visible light photocatalytic inactivation of *Escherichia coli* with combustion synthesized TiO_2, *Chem. Eng. J.,* 189-190, 101–107.

[12] Pelaez, M., Nolan, N.T., Pillai, S.C., Seery, M.K., Falaras, P., Kontos, A.G., Dunlop, P.S.M., Hamilton, J.W.J., Byrne, J.A., O'Shea, K., Entezari, M.H., and Dionysiou, D.D., 2012, Review on the visible light active titanium dioxide photocatalysts for environmental applications, *Appl. Catal., B,* 125, 331–349.

[13] Suwarnkar, M.B., Dhabbe, R.S., Kadam, A.N., and Garadkar, K.M., 2014, Enhanced photocatalytic activity of Ag doped TiO_2 nanoparticles synthesized by a microwave assisted method, *Ceram. Int.,* 40 (4), 5489–5496.

[14] Kernazhitsky, L., Shymanovska, V., Gavrilko, T., Naumov, V., Fedorenko, L., Kshnyakin, V., and Baran, J., 2014, Room temperature photoluminescence of anatase and rutile TiO_2 powders, *J. Lumin.,* 146, 199–204.

[15] Lenzi, G.G., Fávero, C.V.B., Colpini, L.M.S., Bernabe, H., Baesso, M.L., Specchia, S., and Santo, O.A.A., 2011, Photocatalytic reduction of Hg(II) on TiO_2 and Ag/TiO_2 prepared by the sol–gel and impregnation methods, *Desalination,* 270 (1-3), 241–247.

[16] Susanthy, D., Santosa, S.J., and Kunarti, E.S., 2020, Antibacterial activity of silver nanoparticles capped by *p*-aminobenzoic acid on *Escherichia coli* and *Staphylococcus aureus, Indones. J. Chem.,* 20 (1), 182–189.

[17] Susanthy, D., Santosa, S.J., and Kunarti, E.S., 2018, The synthesis and stability study of silver nanoparticles prepared using *p*-aminobenzoic acid as reducing and stabilizing agent, *Indones. J. Chem.,* 18 (3), 421–427.

[18] Roto, R., Marcelina, M., Aprilita, N.H., Mudasir, M., Natsir, T.A., and Mellisani, B., 2017, Investigation on the effect of addition of Fe^{3+} ion into the colloidal AgNPs in PVA solution and understanding its reaction mechanism, *Indones. J. Chem.,* 17 (3), 439–445.

[19] Roto, R., Rasydta, H.P., Suratman, A., and Aprilita, N.H., 2018, Effect of reducing agents on physical and chemical properties of silver nanoparticles, *Indones. J. Chem.,* 18 (4), 614–620.

[20] Zhao, Y., Sun, L., Xi, M., Feng, Q., Jiang, C., and Fong, H., 2014, Electrospun TiO_2 nanofelt surface-decorated with Ag nanoparticles as sensitive and UV-cleanable substrate for surface enhanced Raman scattering, *ACS Appl. Mater. Interfaces,* 6 (8), 5759–5767.

[21] Albiter, E., Valenzuela, M.A., Alfaro, S., Valvelde-Aguilar, G., and Martinez-Pallares, F.M., 2015, Photocatalytic deposition of Ag nanoparticles on TiO$_2$: Metal precursor effect on the structural and photoactivity properties, *J. Saudi Chem. Soc.*, 19 (5), 563–573.

[22] Flanagan, J.N., and Steck, T.R., 2017, The relationship between agar thickness and antimicrobial susceptibility testing, *Indian J. Microbiol.*, 57 (4), 503–506.

[23] Fujii, G., Chang, J.E., Coley, T., and Steere, B., 1997, The formation of amphotericin B ion channels in lipid bilayers, *Biochemistry*, 36 (16), 4959–4968.

[24] Mei, S., Wang, H., Wang, W., Tong, L, Pan, H., Ruan, C., Ma, Q., Liu, M., Yang, H., Zhang, L., Cheng, Y., Zhang, Y., Zhao, L., and Chu, P.K., 2014, Antibacterial effects and biocompatibility of titanium surfaces with graded silver incorporation in titania nanotubes, *Biomaterials*, 35, 4255–4265.